Polytope 335 and the Qi Men Dun Jia Model

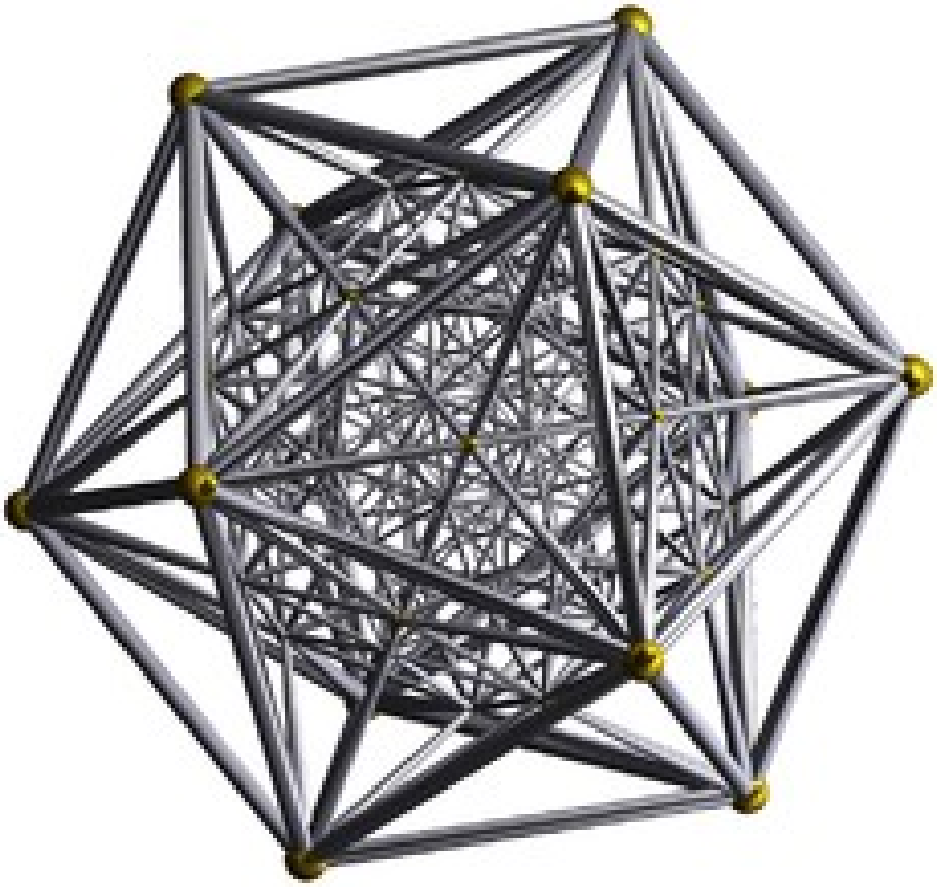

By John Frederick Sweeney

Abstract

Polytope (3,3,5) plays an extremely crucial role in the transformation of visible matter, as well as in the structure of Time. Polytope (3,3,5) helps to determine whether matter follows the 8 x 8 Satva path or the 9 x 9 Raja path of development. Polytope (3,3,5) on a micro scale determines the development path of matter, while Polytope (3,3,5) on a macro scale determines the geography of Time, given its relationship to Base 60 math and to the icosahedron. Yet the Hopf Fibration is needed to form Poytope (3,3,5). This paper outlines the series of interchanges between root lattices and the three types of Hopf Fibrations in the formation of quasi – crystals.

Table of Contents

Introduction

This paper introduces the formation of Polytope (3,3,5) and the role of the Real Hopf Fibration, the Complex and the Quarternion Hopf Fibration in the formation of visible matter. The author has found that even degrees or dimensions host root lattices and stable forms, while odd dimensions host Hopf Fibrations. The Hopf Fibration is a necessary structure in the formation of Polytope (3,3,5), and so it appears that the three types of Hopf Fibrations mentioned above form an intrinsic aspect of the formation of matter via root lattices.

This paper follows the work of R.B King, as well as Lord and Jaganathan, to illustrate the formation and features of Polytope (3,3,5), which plays a crucial role in higher forms of matter. At the same time, Quarternions play a key role in the formation of Polytope (3,3,5), especially along its vertices and symmetry group.

The third section of this paper discusses the isometric relations of H3 and H4 with a section from King, as well as a piece by John Baez. The isometric relations described here play an important role in determining whether matter takes the stable 8 x 8 Satva course, or the more dynamic 9 x 9 Raja course.

Finally, this paper attempts to account for the process of the formation of matter in each dimension, with a chart that shows the key features of each dimension.

3 The polytope {3, 3, 5}

Perfectly regular tetrahedra can be packed together in a spherical space S_3. On a hypersphere embedded in Euclidean space E_4 the vertices are those of the regular polytope $\{3, 3, 5\}$. It follows that various of the clusters discussed above, built from slightly irregular tetrahedra, exist in this polytope without any irregularity.

The polytope $\{3, 3, 5\}$ has 120 vertices, 720 edges, 1200 equilateral triangular faces and 600 regular tetrahedral cells [22]. There are 5 tetrahedra around every edge and twelve around every vertex (forming a regular icosahedron). From these facts, the information contained in the incidence matrix below is easily deduced. The off-diagonal element ij gives the number of $(j-1)$-dimensional "facets" contained in or containing each $(i-1)$-dimensional facet:

120	12	30	12
2	720	5	5
3	3	1200	2
4	6	4	600

A standard set of coordinates for the vertices is given by all the *even* permutations of

$$\begin{aligned} \frac{1}{2}\left(\pm 2\ 0\ 0\ 0\right) \\ \frac{1}{2}\left(\pm 1\ \pm 1\ \pm 1\ \pm 1\right) \\ \frac{1}{2}\left(\pm \tau\ \pm 1\ \pm \sigma\ 0\right) \end{aligned} \tag{3.1}$$

where τ is the golden number, $\tau = (1+\sqrt{5})/2$ and $\sigma = -\tau^{-1} = (1-\sqrt{5})/2$ (*i.e.*, τ and σ are the roots of $\lambda^2 - \lambda - 1 = 0$). The radius of this $\{3, 3, 5\}$ is 1 and its edge length is $1/\tau$.

The vertices, of course, all lie on the *hypersphere* (S_3)

$$x_0^2 + x_1^2 + x_2^2 + x_3^2 = 1. \tag{3.2}$$

Table 1. Radii of successive shells around a vertex of $\{3, 3, 5\}$.

$2x_0$	n		d	$\cos\alpha$
2	1	"centre"	0	1
τ	12	icosahedron	$1/\tau$	τ
1	20	dodecahedron	1	$1/2$
$-\sigma$	12	icosahedron	$\sqrt{(3-\tau)}$	$1/2\tau$
0	30	icosidodecahedron	$\sqrt{2}$	0
σ	12	icosahedron	τ	$-1/\tau$
-1	20	dodecahedron	$\sqrt{3}$	$-1/2$
$-\tau$	12	icosahedron	$\sqrt{(2+\tau)}$	$-\tau/2$
-2	1	antipodal vertex	2	-1

Table 2. Coordinates of the vertices of the icosidodecahedral shell indicated in Figure 12.

1	2	3	4	5	6	7	8	9	10	11	12	13	14	15
$-\sigma$	1	τ	2	0	0	σ	1	τ	τ	$-\sigma$	-1	τ	σ	-1
τ	$-\sigma$	1	0	2	0	τ	σ	1	-1	τ	$-\sigma$	-1	τ	σ
1	τ	$-\sigma$	0	0	2	1	τ	σ	$-\sigma$	-1	τ	σ	-1	τ

The Hopf Fibration

In the next section, it becomes readily apparent, although understated, that the Hopf Fibration plays a key role in the development of Polytope (3,3,5). Given their similarities in structure, it may prove the case that the Bloch Sphere plays an analogous role in nuclear physics, yet on a different scale. The Hopf Fibration is also known as the Hopf Map and the Hopf Fibre Bundle or the Hopf Bundle – the various aliases the structure takes on across mathematical physics, including S3, here.

As this version includes the Quarternions, we may probably assume that the version described here is the Quarternionic Hopf Fibration. Quarternions play a crucial role in the formation of Polytope (3,3,5).

In the spherical representation of the polytope the edges, faces and cells are projected onto this S_3. The edges are then represented by arcs of *great circles*. A way of visualising the polytope is as follows [22]. Take a single vertex – for convenience, (1 0 0 0) – as a "centre" and consider the successive "shells" of vertices that surround it. The first shell is an icosahedron, then 12 vertices lying over the faces of the first shell form a regular dodecahedron. The third shell is another, larger icosahedron. So far, the sequence is the same as the sequence of shells of atoms in the Bergman cluster [25]. The vertices of the next shell all lie on a *great sphere* of the S_3 (in the lower dimensional analogy, the "centre" would be, say, the north pole. We have arrived at the equator). This great sphere contains 30 vertices, forming an *icosidodecahedron* (*i.e.* the Archimedean polyhedron whose vertices are all the midpoints of edges of an icosahedron. Its triangular and pentagonal faces are arranged in the pattern (3.5.3.5) around the vertices). The sequence of shells thereafter goes in reverse order, till we reach (−1 0 0 0) (the "south pole"). Table 1 gives, for each shell, the x_0 coordinate of its vertices, its distance d from the (1 0 0 0) measured in E_4, and its distance α measured in S_3.

In the following section it will be convenient to have names (labels) for the vertices of the equatorial icosidodecahedron. Our labelling system is given by Table 2, which lists, for each vertex, the coordinates $2x_1$, $2x_2$, $2x_3$ (as a column).

The vertices diametrically opposite those listed may be denoted by attaching minus signs to the labels. The labelling of the icosidodecahedron is illustrated in Figure 12.

Observe that the edges and vertices of an icosidodecahedron lie on *six planar decagons*. In the spherical representation, these decagons are *great circles*. The $\{3, 3, 5\}$ contains 72 of them – corresponding to 72 great circles in S_3. It is not difficult to deduce that the vertices, great

circles and great spheres in the spherical representation of $\{3,3,5\}$ constitute a configuration described by the following incidence matrix:

120	6	15
10	72	5
30	6	60

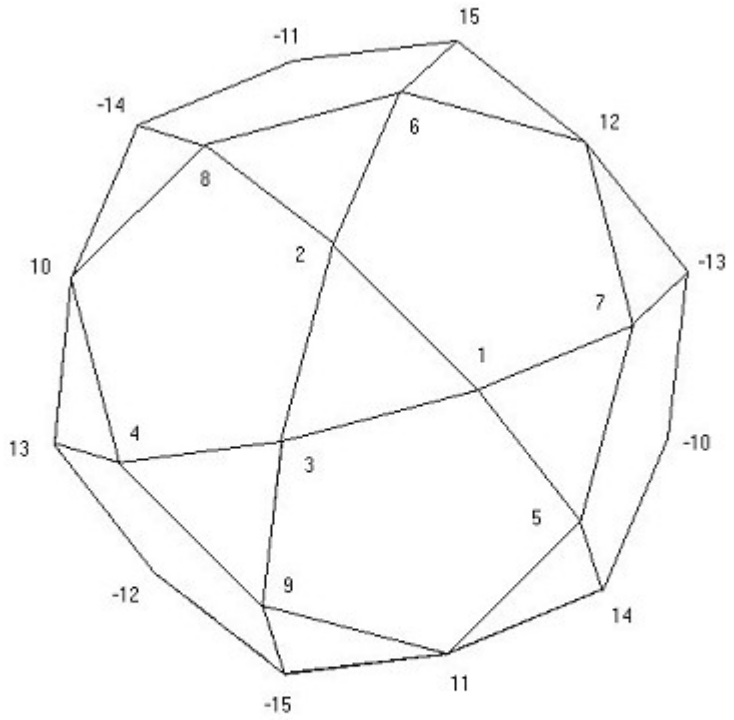

(b)

Fig. 12. The labeling of an equatorial icosidodecahedron of $\{3,3,5\}$. (a) View along 5-old axis. (b) View along 3-fold axis.

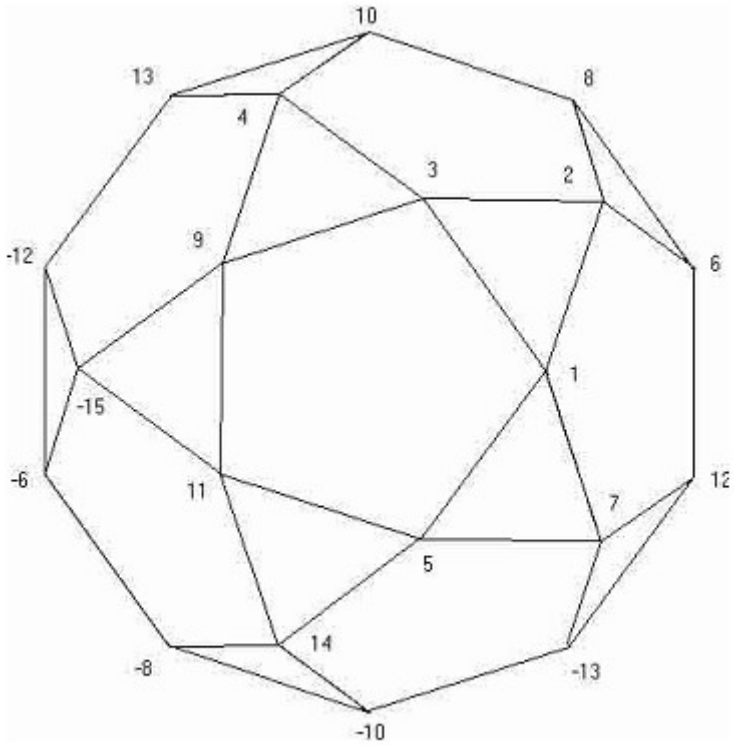

(a)

4 Rotations and double rotations in E_4

Euclidean transformations in E_4 about a fixed origin (equivalently, rotations of S_3) are most simply and elegantly expressed in terms of *quaternions*. "Real" quaternions are essentially sets of four real numbers $q = (q_0\ q_1\ q_2\ q_3) = (q_0, \mathbf{q})$, with the multiplication law

$$pq = (p_0 q_0 - \mathbf{p}\cdot\mathbf{q},\ \mathbf{p}\times\mathbf{q} + p_0\mathbf{q} + \mathbf{p}q_0). \qquad (4.1)$$

The *conjugate* of a quaternion q is $\bar{q} = (q_0, \ -\mathbf{q})$, its *norm* is $q\bar{q} = \bar{q}q = q_0^2 + q_1^2 + q_2^2 + q_3^2$, and its *modulus* $|q|$ is the square root of the norm. The *unit quaternion* is (1 0 0 0) and every non-zero quaternion has an inverse $q^{-1} = \bar{q}/|q|$.

Writing the coordinates of points in E_4 as quaternions $x = (x_0 \ x_1 \ x_2 \ x_3) = (x_0, \mathbf{x})$, the Euclidean transformations, keeping the origin fixed are the *double rotations*

$$x \to pxq, \tag{4.2}$$

where p and q are quaternions of unit norm. The corresponding orthogonal 4×4 matrix is

$$R = PQ, \tag{4.3}$$

where

$$P = \begin{pmatrix} p_0 & -p_1 & -p_2 & -p_3 \\ p_1 & p_0 & p_3 & -p_2 \\ p_2 & -p_3 & p_0 & p_1 \\ p_3 & p_2 & -p_1 & p_0 \end{pmatrix}, \quad Q = \begin{pmatrix} q_0 & -q_1 & -q_2 & -q_3 \\ q_1 & q_0 & -q_3 & q_2 \\ q_2 & q_3 & q_0 & -q_1 \\ q_3 & -q_2 & q_1 & q_0 \end{pmatrix}.$$

The quaternions p and q can be written as

$$p = (\cos\theta, \ \mathbf{n}\sin\theta), \qquad q = (\cos\varphi, \ \mathbf{m}\sin\varphi), \tag{4.4}$$

thus defining a useful set of parameters for the four-dimensional orthogonal group: two angles θ and φ and two unit 3-vectors $\mathbf{n}$ and $\mathbf{m}$.

The special transformations of the form

$$x \to px, \qquad \text{and} \quad x \to xq \tag{4.5}$$

are called, respectively, *left* and *right Clifford translations*. In their action on a hypersphere S_3, centred at the origin of E_4, they have *no fixed points* (this phenomenon has no analogue in E_3: every rotation of a sphere S_2 has two fixed points). This observation leads to the concept of a *Hopf fibration* [16,26] of S_3. For any given point x in S_3, a transformation $x \to px$ generates a *great circle* in S_3, parametrised by the variable θ. For fixed $\mathbf{n}$, we can generate a great circle through *every* point x of S_3. This set of circles constitute a *left Hopf fibration*. Obviously, no two of the circles can intersect. In fact, every pair of circles is linked! The circles are the *fibres* of the fibration. Similarly, *right Hopf fibrations* are defined in terms of the transformations $x \to xq$.

5 Rotational symmetries of $\{3, 3, 5\}$

The symmetries of $\{3, 3, 5\}$ are transformations of the form (4.3) for which the components of p and q are permutations of the coordinate sets (3.1). We get a group of order 7 200. (The full symmetry group including reflections has order 14 400). It is a strange property of the polytope $\{3, 3, 5\}$ that the quaternions representing its vertices are the same quaternions that represent its symmetries. Even more odd is that the rows and columns of the 7 200 matrices R are the same 120 4-vectors!

Left and Right Clifford Translations

Spherical space S_3 can be parametrised by three angular variables (analogous to longitude and latitude, for S_2):

$$\begin{aligned} x_0 &= \sin\Theta\cos\Phi, \quad & x_1 &= \cos\Theta\cos\Psi, \\ x_2 &= \cos\Theta\sin\Psi, \quad & x_3 &= \sin\Theta\sin\Phi. \end{aligned} \tag{8.1}$$

Observe that $\Phi \to \Phi + \alpha$ is a rotation in the (0 3)-plane and $\Psi \to \Psi + \beta$ is a rotation in the (1 2)-plane. In terms of quaternions, these transformations are respectively $x \to pxp$ and $x \to px\bar{p}$, with $p = (\cos(\alpha/2),\ 0,\ 0,\ \sin(\alpha/2))$. It follows that, in terms of these polar coordinates,

$$\Phi \to \Phi + \gamma, \quad \Psi \to \Psi - \gamma \tag{8.2}$$

is a *left Clifford translation* and

$$\Phi \to \Phi + \gamma, \quad \Psi \to \Psi + \gamma \tag{8.3}$$

is a *right Clifford translation*. (In terms of quaternions, $x \to px$ and $x \to xq$, respectively, with p or q of the form $(\cos\gamma, 0, 0, \sin\gamma)$).

The 120 vertices of $\{3,3,5\}$ lie in tens on 12 great circles, which are twelve circles of a Hopf fibration. In fact, the vertices can be assigned in tens to twelve fibres, in 24 different ways (corresponding to 12 left and 12 right fibrations. Consider, for definiteness, the effect of the left translation $p \to px$ with

$$p = \frac{1}{2}(\tau \ -\sigma \ 1 \ 0), \tag{5.1}$$

(*i.e.*, $\theta = \pi/5$ and $\mathbf{n} \sim [1 \ \tau \ 0]$) on the vertices of the polytope. In matrix formulation, we have the repeated action of the corresponding orthogonal matrix

$$R = \frac{1}{2}\begin{pmatrix} \tau & \sigma & -1 & 0 \\ -\sigma & \tau & 0 & -1 \\ 1 & 0 & \tau & -\sigma \\ 0 & 1 & \sigma & \tau \end{pmatrix} \tag{5.2}$$

on the position vectors. Since $p^5 = -1$, R has order 10, so it generates decagons. The repeated action of R on any vertex of the polytope generates a decagon of vertices lying on a fibre.

The twelve fibres can be visualised in terms of a stereographic projection of S_3 to E_3. Since E_3 is the space in which we live, configurations in it are more easily imagined. Moreover, circles in S_3 are mapped to circles (or straight lines) in E_3 and spheres are mapped to spheres (or planes). Let us project from $(-1\ 0\ 0\ 0)$ to the hyperplane (E_3) $x_0 = 0$.

Starting from vertex **6** $(0\ 0\ 0\ 1)$ and applying the transformation R repeatedly we get the sequence of ten vertices around the perimeter of Figure 12b – lying on a great circle **A**. Starting from $(1\ 0\ 0\ 0)$ we get a great circle **B** – which in the stereogram is a line perpendicular to the page passing through the middle of the figure, containing none of the vertices of the icosidodecahedron. The remaining 10 fibres are obtained by repeated application of R to the remaining ten vertices of the icosidodecahedron. They are circles that pass through a pair of diametrically opposite vertices of the icosidodecahedron.

Similarly, a fibration $x \to xq$ with $\varphi = \pi/3$ (so that $q^3 = -1$) gives a transformation of order six that assigns the 120 vertices of the polytope to 20 fibres with six vertices on each. The hexagon edges, however, are not edges of the $\{3,3,5\}$

6 The Boerdijk-Coxeter helices in $\{3, 3, 5\}$

Consider the effect of repeated action of

$$x \to p^2 x q \tag{6.1}$$

with $p = 1/2(\tau\ -\sigma\ 1\ 0)$, $q = 1/2(1\ 1\ 1\ 1)$; *i.e.*, $\theta = \pi/5$, $\varphi = \pi/3$, $\mathbf{n} \sim [1\ \tau\ 0]$, $\mathbf{m} \sim [1\ 1\ 1]$. Then

$$R = \frac{1}{2}\begin{pmatrix} -1 & -\tau & \sigma & 0 \\ 0 & -\sigma & -\tau & -1 \\ \tau & -1 & 0 & \sigma \\ -\sigma & 0 & -1 & \tau \end{pmatrix}. \tag{6.2}$$

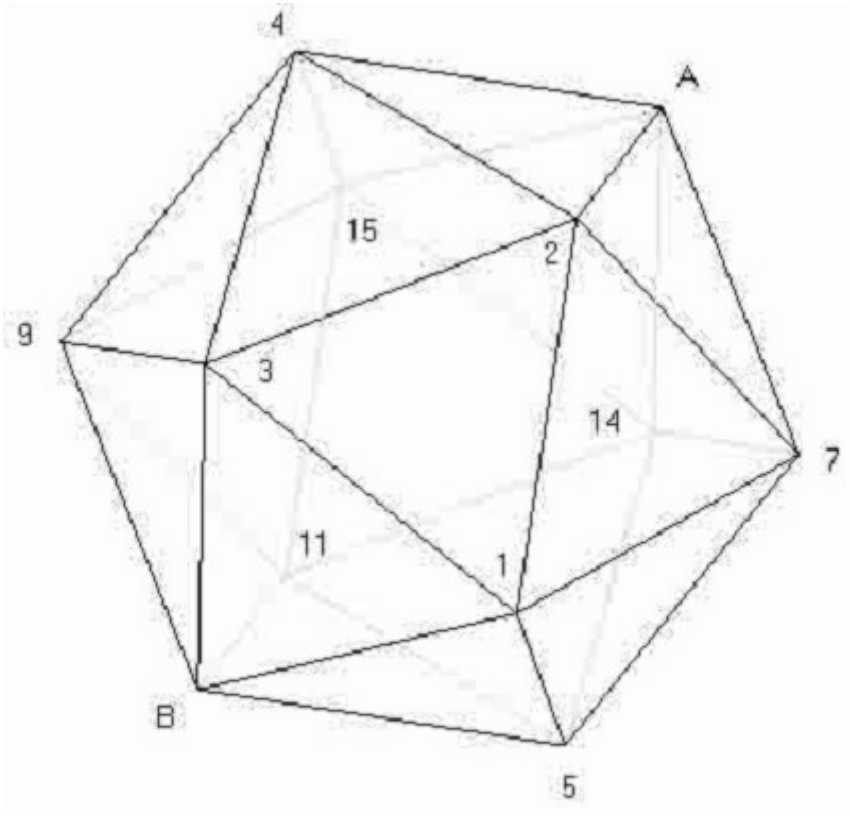

Fig. 13. Representation of the configuration of twelve fibres of a Hopf libration.

Since $p^5 = q^3 = -1$, R has order 30. It will generate a sequence of 30 vertices (an orbit of the transformation R), starting from any vertex of $\{3,3,5\}$. For example, starting from **6** (0 0 0 1) we get the the vertices given by the columns of

$$\frac{1}{2}\begin{pmatrix} 0 & 0 & 1 & 0 & -\sigma & 1 & 0 & 1 & -\sigma & 0 & 1 & 0 & 0 & -\sigma & \sigma & \\ 0 & -1 & \sigma & -1 & -\tau & -1 & -\tau & -\tau & -1 & -\tau & -1 & \sigma & -1 & 0 & 0 & \\ 0 & \sigma & 0 & -\sigma & 0 & 1 & 1 & -\sigma & \tau & 1 & 1 & \tau & -\sigma & 1 & 1 & \ldots \\ 2 & \tau & \tau & \tau & 1 & 1 & -\sigma & 0 & 0 & \sigma & -1 & -1 & -\tau & -\tau & -\tau & \end{pmatrix}$$

(... denotes a repetition of the fifteen given columns, with opposite sign.) in this sequence, every set of four consecutive vertices is the set of vertices of a regular tetrahedron with edge length $1/\tau$. That is, we have a *Boerdijk-Coxeter helix* consisting of 30 tetrahedral cells of $\{3,3,5\}$.

The geometrical situation can be explored further. The fibres of a Hopf fibration are *parallel* (*i.e.*, any two maintain a constant S_3 distance from each other). Each of the twelve fibres associated with the decagons of $\{3,3,5\}$ has five nearest neighbours. Figure 13 is a representation of this nearest neighbour relationship. The twelve fibres are represented as the twelve vertices of an icosahedron and the icosahedron edges represent the nearest neighbour relationship. (N.B.: this icosahedron has nothing to do with the icosahedral shells of the polytope. In the mathematical terminology it is the *base space* of the *fibre bundle* [26].) For every triangular face of this icosahedron there is a B-C helix whose type $\{3\}$ helices are three decagons of the polytope. Thus $\{3,3,5\}$ consists of twenty toroidal B-C helices packed together, wrapped around each other.

TABLE I. Properties of the regular (Platonic) polyhedra

Polyhedron	Face type	Vertex degrees	Number of edges	Number of faces	Number of vertices
Tetrahedron {3,3}	Triangle	3	6	4	4
Octahedron {3,4}	Triangle	4	12	8	6
Cube {4,3}	Square	3	12	6	8
Icosahedron {3,5}	Triangle	5	30	20	12
Dodecahedron {5,3}	Pentagon	3	30	12	20

To obtain a realistic model for the collagen structure by projection from the corresponding structure in $\{3,3,5\}$ a mapping is required that maps great circles of a Hopf fibration of S_3 to *helices* in E_3. In terms of the polar coordinate system given by (8.1), a mapping with this property exists that has a remarkably simple form. Let ρ, φ, z be the coordinates of a cylindrical coordinate system in E_3. Then the mapping from S_3 to E_3 given by

$$\rho = \Theta, \quad \varphi = \Phi, \quad z = -\Psi \tag{8.4}$$

has the following properties. The fibres of the left translation (8.2) all lie on toruses $\Theta = const.$ and are mapped to helices that wind around the z-axis (which is itself the image of the fibre $\Theta = 0$). Distances along the z-axis and radial distances from the z-axis represent accurately the corresponding distances in S_3. The projection is a generalisation to higher dimensions of *Mercator's projection* from S_2 to E_2, which represents distances along the equator and along lines of longitude accurately to scale, while stretching out of lines of latitude increases in severity as one moves away from the equator.

We now choose the position of a $\{3,3,5\}$ in S_3 so that all the vertices of one of its B-C helices lie on a torus $\Theta = const.$ (and hence the projected vertices in E_3 all lie on a cylinder whose axis is the z-axis). The minus sign in (8.4) ensures that the type $\{1\}$ helix will be right-handed.

We have seen that the 30 vertices of a type $\{1\}$ helix in S_3 are generated by a transformation P^2Q, where P is a left translation with angular parameter $\pi/5$ and Q is a right translation with angular parameter $\pi/3$. It follows from the prescriptions (8.2, 8.3), that such a transformation is given by

$$\Phi \to \Phi + 11\pi/15, \qquad \Psi \to \Psi - \pi/15. \tag{8.5}$$

The image of a point $(\Theta, \Phi, \Psi) = (\Theta_1, 0, 0)$ is $(\Theta_1, 11\pi/15, -\pi/15)$. If these are two vertices of an edge of $\{3,3,5\}$ their S_3 distance must be $\cos^{-1}(\tau/2)$. This gives

$$\tau/2 = \sin^2\Theta_1 \cos(11\pi/15) + \cos^2\Theta_1 \cos(\pi/15),$$

and hence

$$\cos\Theta_1 = \sqrt{\frac{1}{2}\left(1 + \frac{\tau^2}{\sqrt{3(2+\tau)}}\right)}. \qquad (8.6)$$

This enables the polar coordinates of all the vertices of a B-C helix in $\{3,3,5\}$ (and hence their images in E_3) to be computed. To identify the positions of other vertices of this $\{3,3,5\}$ we proceed as follows:

Let v_1, v_2, v_3, v_4 be the E_4 position vectors of the vertices of any tetrahedral cell of our $\{3,3,5\}$ and let v_5 be the position vector of the remaining vertex of the adjoining cell, sharing the face (v_1, v_2, v_3). Then

$$v_5 = (v_1 + v_2 + v_3)/\tau - v_4. \qquad (8.7)$$

(Observe, incidentally, that the corresponding formula for a pair of tetrahedra lying in E_3 is $v_5 = \frac{2}{3}(v_1+v_2+v_3) - v_4$. To produce the polytope, contiguous tetrahedra are rotated about their common face – just as, in making a model of an icosahedron from a flat net, we have to rotate neighbouring triangles about their common edge.)

In principle, the positions of all 120 vertices of a $\{3,3,5\}$ can be computed from this formula, if the positions of the three vertices of a single triangular face are given.

The central type $\{1\}$ helix obtained by the projection of $\{3,3,5\}$ employing (8.4) is an almost exact Coxeter helix: the number of edges per turn is $30/11 = 2.727$, instead of 2.731. The structure is periodic − the type $\{3\}$ helix has exactly 10 edges per turn. a slight "untwisting" of this structure is still required if a realistic model of the collagen model is to be obtained. We apply a further transformation of the form $\varphi \to \varphi + kz$. the parameter k adjusts the pitch of the type $\{3\}$ helices of the central B-C structure, and is chosen so that about ten glycines per turn occur along each type $\{3\}$ helix of the core, as in the actual molecule. This untwisting transformation introduces very slight additional deformation of the central B-C helix, but *lessens* the inevitable distortion of the three outer B-C helices.

R. B King on Root Lattices and Quasi – Crystals

R. B. King explains directly the process of how quasi-crystals develop from root lattices in even dimensions, and his method of explanation does not require the Lie Algebras or the Exceptional Lie Algebras. Instead, King chooses the less – traveled path, describing the formation of three – dimensional icosahedral quasi – crystals. King's method reflects the path taken in this series of papers published exclusively on Vixra, which trace the path of the development of visible matter along the lines of Platonic Solids.

ROOT LATTICES FROM REFLECTION GROUPS

In order to provide a clearer geometric picture, this paper derives root lattices from reflection groups[10] rather than from Lie groups.[11] In this connection consider a kaleidoscope whose three mirrors (or walls) cut the sphere in a spherical triangle having angles $\pi/2$, $\pi/3$, and $\pi/5$ (Figure 4a). The reflections in these walls generate a group of order 120 called the H_3 reflection group. The whole surface of the sphere is divided into 120 triangles, one for each group element. In this specific example the H_3 reflection group is isomorphic to the icosahedral point group I_h.

Here King explains his reasoning for choosing reflection groups over Lie Groups, and then introduces the H3, of order 120, which is isomorphic to the icosahedral point group Ih. In fact, we shall see that the reflection groups H2, H3 and H4 hold isomorphic relations with other key groups in the critical region where matter transforms either into stable 8 x 8 Satva forms or into dynamic 9 x 9 Raja forms.

Next, King goes on to explain the concept of tessellation and its importance to the formation of quasi-crystals. From the point of view of the Qi Men Dun Jia Model, King's discussion of tessellation helps to explain why the Platonic Solids play a key role in the formation, while at the same time helping to explain the omni – presence of the Golden Ratio throughout the process of the formation of matter – no mere coincidence, but a necessary element in the process.

The concept of a tessellation is useful for generating regular polytopes of low dimension as well as related lattices. In this connection, embedding a network of polygons into a surface can be described as a tiling or tessellation of the surface.[15] In a formal sense a tiling or tessellation of a surface is a countable family of closed sets T = $\{T_1,T_2\ldots\}$ which cover the surface without gaps or overlaps. More explicitly, the union of the sets $T_1,T_2\ldots$ (which are known as the tiles of T) is the whole surface and the interiors of the sets T_i are pairwise disjoint. In the tessellations of interest in this paper, the tiles are the polygons, which, in the case of tessellations corresponding to polyhedra, are the faces of the polyhedra. Tessellations can be described in terms of their flags, where a flag is a triple (V, E, F) consisting of a vertex V, and edge E, and a face F which are mutually incident. A tiling T is called regular if its symmetry group G(T) is transitive on the flags of T. A regular tessellation consisting of q regular p-gons at each vertex can be described by the so-called Schäfli notation $\{p,q\}$. The Schäfli notation can be generalized to higher dimensions in the obvious way.

The dual pairs for the Platonic polyhedra consist of the cube/octahedron and dodecahedron/icosahedron (Figure 1). The tetrahedron is self-dual, *i.e.*, the dual of a tetrahedron is another tetrahedron. Also the concept of duality can be extended from standard polyhedra embedded in the surface of a sphere to polygonal networks embedded in surfaces of non-zero genus. In this connection the author has studied

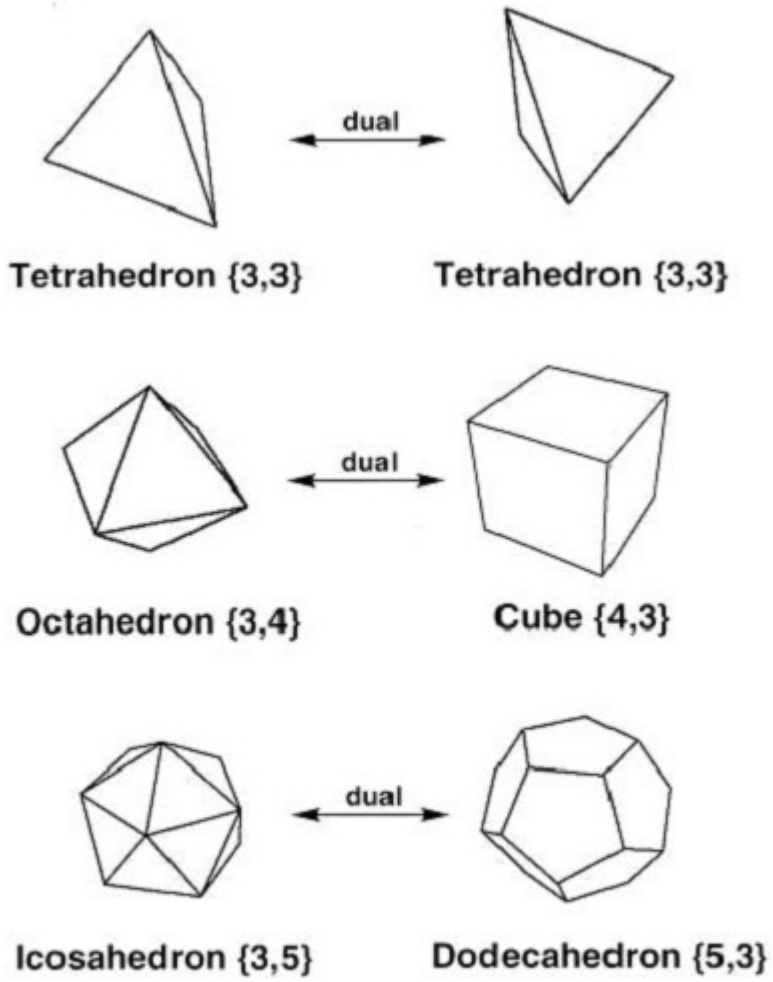

Figure 1. The five regular »Platonic« polyhedra showing their Schäfli symbols and the dual pairs. Note that the tetrahedron is self-dual.

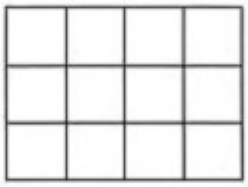

{4,4} ("checkerboard plane")

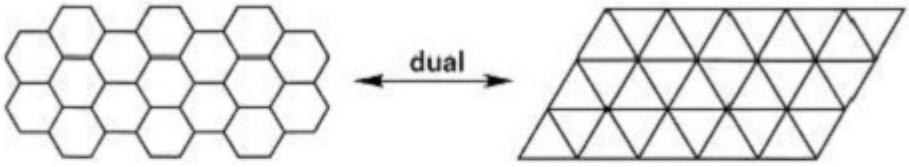

{6,3} ("graphite structure") {3,6} tessellation

Figure 2. The three regular tessellations of the plane, namely the self-dual {4,4} checkerboard tessellation and the {6,3}↔{3,6} dual pair.

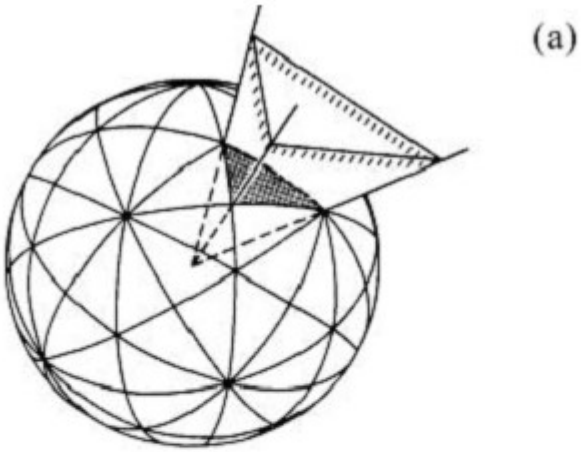

The H_3 reflection group

Figure 4. (a) Generation of the H_3 reflection group ($\approx I_h$ point group); (b) The Coxeter-Dynkin diagram for the H_3 reflection group.

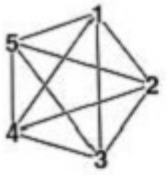

{3,3,3}

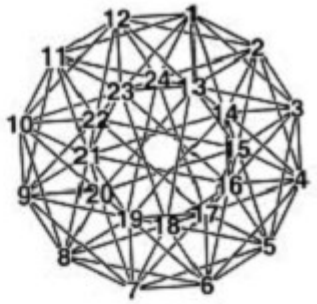

{3,4,3}

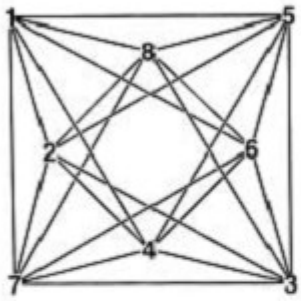

{3,3,4}

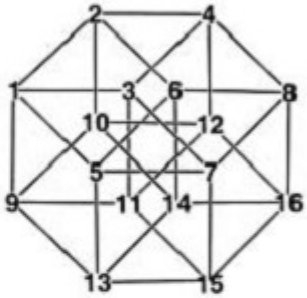

{4,3,3}

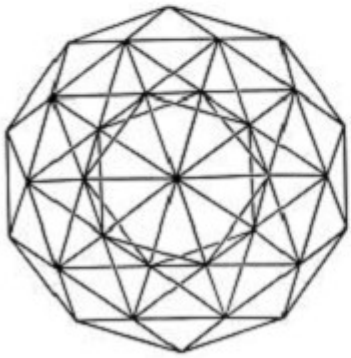

{3,3,5}

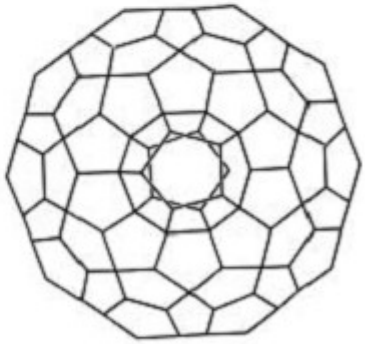

{5,3,3}

Figure 3. Projections of the six regular four-dimensional polytopes and their Schäfli symbols. For clarity only the »front« portions of the large {3,3,5} and {5,3,3} polytopes are shown.

H3 & H4 Reflection Groups

In this section we include King's discussion of these two important reflection groups as well as John Baez's take on the same. Their isomorphic relations play a key role in the process of the development of visible matter, before the shift to 8 x 8 or 9 x 9 types of matter.

The group H_3 is an example of a finite or spherical reflection group. Such groups are called irreducible if they cannot be generated by direct products of smaller irreducible groups. In general, such irreducible reflection groups are generated by reflections in the walls of a spherical simplex, all of whose dihedral angles are submultiples of π. The infinite cone bounded by the reflecting walls or hyperplanes (*i.e.*, the kaleidoscope) is a fundamental region of the reflection group. If R_i is the reflection in the ith wall of the fundamental region, a set of generating relations for the corresponding reflection group can be generated by the following set of defining relations:

$$R_i^2 = (R_i\, R_j)^{p_{ij}} = 1 \ (i, j = 1,\ldots,n) \qquad (1)$$

In Eq. (1) π/p_{ij} is the angle between the ith and jth walls. Coxeter has proven that every finite group with a set of defining relations of this form is a reflection group. Such reflection groups can be described by a Coxeter-Dynkin diagram, which has one vertex for each wall with two vertices being joined by a line labeled with the exponents p in the defining relations (Eq. 1). Certain abbreviations are customarily used for lines labelled with small values of p, as shown in Figure 5a. The Coxeter-Dynkin diagram for the reflection group H_3 is given in Figure 4b.

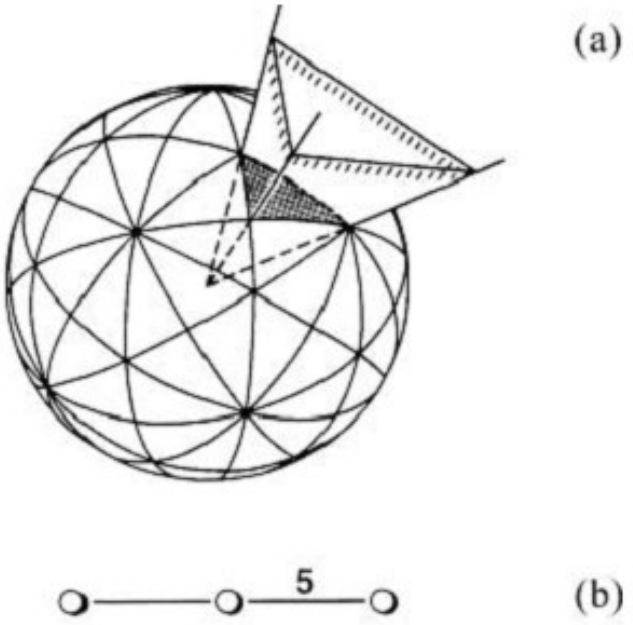

Figure 4. (a) Generation of the H_3 reflection group ($\approx I_h$ point group); (b) The Coxeter-Dynkin diagram for the H_3 reflection group.

Of particular interest in connection with the theory of icosahedral quasicrystals to be discussed in this paper is the fact that the regular icosahedron has a four-dimensional analogue, namely the {3,3,5} polytope, but no regular polytope analogues beyond four dimensions.

The group H_3 as noted above (Figure 4) corresponds to the symmetry point group I_h of the regular icosahedron {3,5} or its dual, namely the regular dodecahedron {5,3} (Figure 1). Similarly the group H_4 corresponds to the four-dimensional symmetry point group of the regular four-dimensional polytope {3,3,5} or its dual {5,3,3} (Figure 3).

TABLE II. The indecomposable finite root systems

Root system	Lattice	Number of root vectors	Construction
A_n	A_n	$n(n+1)$	Projection of $\boldsymbol{e}_i - \boldsymbol{e}_j$ (i, j = 1 to n–1) into n-space
B_n	Z^n	$2n^2$	$\{\pm\boldsymbol{e}_i, \pm\boldsymbol{e}_i \pm \boldsymbol{e}_j\}$ where (i, j = 1 to n)
C_n	D_n	$2n^2$	$\{\pm 2\boldsymbol{e}_i, \pm\boldsymbol{e}_i \pm \boldsymbol{e}_j\}$ where (i, j = 1 to n)
D_n	D_n	$2n(n-1)$	$\{\pm\boldsymbol{e}_i \pm \boldsymbol{e}_j\}$ where (i, j = 1 to n)
G_2	A_2	12	$\{(1,0),(^3/_2, ^{\sqrt{3}}/_2)\}$ and six-fold rotations of these points
F_4	D_4	48	$B_4 \oplus \{^1/_2(\pm\boldsymbol{e}_1 \pm \boldsymbol{e}_2 \pm \boldsymbol{e}_3 \pm \boldsymbol{e}_4)\}$
E_6	E_6	72	$A_5 \oplus \{\pm\sqrt{2}\boldsymbol{e}_7, ^1/_2(\pm\boldsymbol{e}_1 \pm \boldsymbol{e}_2 \pm \boldsymbol{e}_3 \pm \boldsymbol{e}_4 \pm \boldsymbol{e}_5 \pm \boldsymbol{e}_6) \pm \boldsymbol{e}_7/\sqrt{2}\}$ with 3+3–
E_7	E_7	126	$A_7 \oplus \{^1/_2(\pm\boldsymbol{e}_1 \pm \boldsymbol{e}_2 \pm \boldsymbol{e}_3 \pm \boldsymbol{e}_4 \pm \boldsymbol{e}_5 \pm \boldsymbol{e}_6 \pm \boldsymbol{e}_7 \pm \boldsymbol{e}_8)\}$ with 4+4–
E_8	E_8	240	$D_8 \oplus \{^1/_2(\pm\boldsymbol{e}_1 \pm \boldsymbol{e}_2 \pm \boldsymbol{e}_3 \pm \boldsymbol{e}_4 \pm \boldsymbol{e}_5 \pm \boldsymbol{e}_6 \pm \boldsymbol{e}_7 \pm \boldsymbol{e}_8)\}$ with even # +

Croat. Chem. Acta **77** (1–2) 133–140 (2004)

John Baez on H3 and H4

7) Andreas Fring and Christian Korff, Non-crystallographic reduction of Calogero-Moser models, Jour. Phys. A 39 (2006), 1115-1131. Also available as hep-th/0509152.

We apply a recently introduced reduction procedure based on the embedding of non-crystallographic Coxeter groups into crystallographic ones to Calogero–Moser systems. For rational potentials the familiar generalized Calogero Hamiltonian is recovered. For the

Hamiltonians of trigonometric, hyperbolic and elliptic types, we obtain novel integrable dynamical systems with a second potential term which is rescaled by the golden ratio. We explicitly show for the simplest of these non-crystallographic models, how the corresponding classical equations of motion can be derived from a Lie algebraic Lax pair based on the larger, crystallographic Coxeter group.

They set up a nice correspondence between some non-crystallographic Coxeter groups and some crystallographic ones:

the H2 Coxeter group and the A4 Coxeter group,
the H3 Coxeter group and the D6 Coxeter group,
the H4 Coxeter group and the E8 Coxeter group.

A Coxeter group is a finite group of linear transformations of R^n that's generated by reflections. We say such a group is "non-crystallographic" if it's not the symmetries of any lattice. The ones listed above are closely tied to the number 5:

H2 is the symmetry group of a regular pentagon.
H3 is the symmetry group of a regular dodecahedron.
H4 is the symmetry group of a regular 120-cell.

Note these live in 2d, 3d and 4d space. Only in these dimensions are there regular polytopes with 5-fold rotational symmetry! Their symmetry groups are non-crystallographic, because no lattice can have 5-fold rotational symmetry.

A Coxeter group is "crystallographic", or a "Weyl group", if it *is* symmetries of a lattice. In particular:

A4 is the symmetry group of a 4-dimensional lattice also called A4.
D6 is the symmetry group of a 6-dimensional lattice also called D6.
E8 is the symmetry group of an 8-dimensional lattice also called E8.

H_3 is the group of symmetries of the dodecahedron or icosahedron. H_4 is the group of symmetries of a regular solid in 4 dimensions which I talked about in "week20". This regular solid is also called the "unit icosians" - it has 120 vertices, and is a close relative of the icosahedron and dodecahedron. One amazing thing is that it itself *is* a group in a very natural way. There are no "hypericosahedra" or "hyperdodecahedra" in dimensions greater than 4, which is related to the fact that the H series quits at this point.

Conclusion

R. B. King mentions a few more points in his key paper, which we shall raise here to emphasize their importance. In a previous paper in this series, the author published a chart which illustrated the facts that the Hopf Fibrations occur only in odd dimensions, that there are different varieties of Hopf Fibrations, and that they appear in alternate dimensions from key lattices. The author shall again post this chart in this paper, but with a few of the holes filled in by topics raised by R. B. King.

First, King notes on page 134 the two – dimensional quasilattices which have rotational symmetries of orders 5, 8, 10 and 12. The presence of these quasilattices helps to explain some of the missing information in the following chart, at least in the previously - published version. By filling in the missing information, we can begin to see the patterns which emerge between the Real, Complex, Quarternionic and Octionic Hopf Fibrations, and the root lattices and lattices associated with Exceptional Lie Algebras, especially in the region between the second Magic Square of G2, B4, F4 and E8, as was noted in an earlier paper in this series.

Then, King notes at in the abstract and in the conclusion of his paper:

> Thus the generation of a two-dimensional quasilattice with seven-fold symmetry requires projection from a six-dimensional root lattice[13] in contrast to a two-dimensional quasilattice with five-fold symmetry (H_2) where projection from the four-dimensional A_4 root lattice is sufficient.

can generate quasicrystals of other symmetries. Four-dimensional root lattices are sufficient for projections to two-dimensional quasicrystals of eight-fold and twelve-fold symmetries. However, root lattices of at least six-dimensions (*e.g.*, the A_6 lattice) are required to generate two-dimensional quasicrystals of seven-fold symmetry. This might account for the absence of seven-fold symmetry in experimentally observed quasicrystals.

This discussion helps to explain the gap found in the seventh dimension of this chart. Even so, Frank “Tony” Smith has shown how action in the seventh dimension, specifically S7 x S7 x G2 leads to G2 in the fourteenth dimension, as Smith has described on his website and as the author has noted in a paper earlier in this series.

Finally, with regard to the ninth degree or dimension, we find that the

Pontryagin class disappears in this location. Wikipedia states:

In mathematics, the **Pontryagin classes** are certain characteristic classes. The Pontryagin class lies in cohomology groups with degree a multiple of four. It applies to real vector bundles.

The vanishing of the Pontryagin classes and Stiefel-Whitney classes of a vector bundle does not guarantee that the vector bundle is trivial. For example, up to vector bundle isomorphism, there is a unique nontrivial rank 10 vector bundle E_{10} over the 9-sphere. (The clutching function for E_{10} arises from the stable homotopy group $\pi_8(O(10)) = \mathbf{Z}/2\mathbf{Z}$.) The Pontryagin classes and Stiefel-Whitney classes all vanish: the Pontryagin classes don't exist in degree 9, and the Stiefel-Whitney class w_9 of E_{10} vanishes by the Wu formula $w_9 = w_1 w_8 + \mathrm{Sq}^1(w_8)$. Moreover, this vector bundle is stably nontrivial, i.e. the Whitney sum of E_{10} with any trivial bundle remains nontrivial. (Hatcher 2009, p. 76)

Pontryagin classes of a manifold

The **Pontryagin classes of a smooth manifold** are defined to be the Pontryagin classes of its tangent bundle.

Novikov proved in 1966 that if manifolds are homeomorphic then their rational Pontryagin classes $p_k(M, \mathbb{Q})$ in $H^{4k}(M, \mathbb{Q})$ are the same.

If the dimension is at least five, there are at most finitely many different smooth manifolds with given homotopy type and Pontryagin classes.

Now, if Pontryagin Classes fail to exist in the ninth dimension or ninth degree, for some inexplicable reason, then there obviously cannot appear their associated smooth manifolds, nor tangent bundles. This helps to explain why the ninth dimension in the chart below appears empty.

In addition, apparently the binary icosahedral group itself lacks a form in the ninth dimension.

Below the reader may find the chart in its entirety on the next page:

This paper has shown the construction of Polytope (3,3,5) and its intimate relation to the three types of Hopf Fibrations, found in even dimensions while root lattices are found in even dimensions. Similarly, division algebras are found in even dimensions. This paper has tried to account for the anomalies found in various dimensions, including the 5^{th}, 7^{th}, 10^{th}, 12^{th}, 14^{th}, and 15^{th}, in order to account for every stage in the process of formation of visible matter, after its emergence from the substratum.

Dim	Number	Lie Algebra	Hopf Fibration	Lattice	Division Algebra	SPIN
1	Real		S1		Div Alg	
2			Z2	Square Lattice	Div Alg	
3	Complex		S3 Hopf			
4		D4			Div Alg	
5				2D Quasi lattices		
6						
7			S7 Hopf			
8	Quarternion		2D Quasi lattices	Root Lattice	Div Alg	
9						
10			2D Quasi lattices			
11						
12			2D Quasi lattices			
13						
14		G2	S7 x S7 x G2			
15			S7 – S15 – S8			
16	Sedenion		Octionic Projective Plane	Laminated Lattice L16		
17						
18						
19						

Appendix

Wikipedia

The 600-cell partitions into 20 rings of 30 tetrahedra each in a very interesting, quasi-periodic chain called the Boerdijk–Coxeter helix. When superimposed onto the 3-sphere curvature it becomes periodic with a period of 10 vertices, encompassing all 30 cells. In addition, the 16-cell partitions into two 8-tetrahedron chains, four edges long, and the 5-cell partitions into a single degenerate 5-tetrahedron chain.

The above fibrations all map to the following specific tilings of the 2-sphere.[4]

In geometry, the **600-cell** (or **hexacosichoron**) is the convex regular 4-polytope, or polychoron, with Schläfli symbol {3,3,5}. Its boundary is composed of 600 tetrahedral cells with 20 meeting at each vertex. Together they form 1200 triangular faces, 720 edges, and 120 vertices. The edges form 72 flat regular decagons. Each vertex of the 600-cell is a vertex of six such decagons.

The mutual distances of the vertices, measured in degrees of arc on the circumscribed hypersphere, only have the values 36° = $\pi/5$, 60° = $\pi/3$, 72° = $2\pi/5$, 90° = $\pi/2$, 108° = $3\pi/5$, 120° = $2\pi/3$, 144° = $4\pi/5$, and 180° = π. Departing from an arbitrary vertex V one has at 36° and 144° the 12 vertices of an icosahedron, at 60° and 120° the 20 vertices of a dodecahedron, at 72° and 108° again the 12 vertices of an icosahedron, at 90° the 30 vertices of an icosadodecahedron, and finally at 180° the antipodal vertex of V. *References:* S.L. van Oss (1899); F. Buekenhout and M. Parker (1998).

The 600-cell is regarded as the 4-dimensional analog of the icosahedron, since it has five tetrahedra meeting at every edge, just as the icosahedron has five triangles meeting at every vertex. It is also called a **tetraplex** (abbreviated from "tetrahedral complex") and **polytetrahedron**, being bounded by tetrahedral cells.

Its vertex figure is an icosahedron, and its dual polytope is the 120-cell.

Each cell touches, in some manner, 56 other cells. One cell contacts each of the four faces; two cells contact each of the six edges, but not a face; and ten cells contact each of the four vertices, but not a face or edge.

In geometry, the **120-cell** (or **hecatonicosachoron**) is the convex regular 4-polytope with Schläfli symbol {5,3,3}.

The boundary of the 120-cell is composed of 120 dodecahedral cells with 4 meeting at each vertex.

It can be thought of as the 4-dimensional analog of the dodecahedron and has been called a **dodecaplex** (short for "dodecahedral complex"), **hyperdodecahedron**, and **polydodecahedron**. Just as a dodecahedron can be built up as a model with 12 pentagons, 3 around each vertex, the *dodecaplex* can be built up from 120 dodecahedra, with 3 around each edge.

The **Davis 120-cell**, introduced by Davis (1985), is a compact 4-dimensional hyperbolic manifold obtained by identifying opposite faces of the 120-cell, whose universal cover gives the regular honeycomb {5,3,3,5} of 4-dimensional hyperbolic space.

Binary Icosahedron

Relation to 4-dimensional symmetry groups

The 4-dimensional analog of the icosahedral symmetry group I_h is the symmetry group of the 600-cell (also that of its dual, the 120-cell). Just as the former is the Coxeter group of type H_3, the latter is the Coxeter group of type H_4, also denoted [3,3,5]. Its rotational subgroup, denoted $[3,3,5]^+$ is a group of order 7200 living in SO(4). SO(4) has a double cover called Spin(4) in much the same way that Spin(3) is the double cover of SO(3). Similar to the isomorphism Spin(3) = Sp(1), the group Spin(4) is isomorphic to Sp(1) × Sp(1).

The preimage of $[3,3,5]^+$ in Spin(4) (a four-dimensional analogue of $2I$) is precisely the product group $2I \times 2I$ of order 14400. The rotational symmetry group of the 600-cell is then

$[3,3,5]^{+} = (2I \times 2I) / \{ \pm 1 \}.$

Various other 4-dimensional symmetry groups can be constructed from $2I$. For details, see (Conway and Smith, 2003).

S3	S2	# of rings	# of cells per ring	Cell Stacking
600-cell {3,3,5}	Icosahedron {3,5}	20	30	Boerdijk–Coxeter helix
120-cell {5,3,3}	Dodecahedron {5,3}	12	10	face stacking
24-cell {3,4,3}	Tetrahedron {3,3}	4	6	face stacking
	Cube {4,3}	6	4	vertex stacking
16-cell {3,3,4}	Dihedron {n,2}	2	8	Boerdijk–Coxeter helix
8-cell {4,3,3}	Dihedron {n,2}	2	4	face stacking
5-cell {3,3,3}	Whole 2-sphere	1	5	Boerdijk–Coxeter helix

Properties

The following tables lists some properties of the six convex regular polychora. The symmetry groups of these polychora are all Coxeter groups and given in the notation described in that article. The number following the name of the group is the order of the group.

Name	Family	Schläfli symbol	Vertices	Edges	Faces	Cells	Vertex figures	Dual polytope	**Symmetry group**	
pentachoron	simplex	{3,3,3}	5	10	10 triangles	5 tetrahedra	tetrahedra	(self-dual)	A_4	120
tesseract	hypercube	{4,3,3}	16	32	24 squares	8 cubes	tetrahedra	16-cell	B_4	384
16-cell	cross-polytope	{3,3,4}	8	24	32 triangles	16 tetrahedra	octahedra	tesseract	B_4	384
24-cell		{3,4,3}	24	96	96 triangles	24 octahedra	cubes	(self-dual)	F_4	1152
120-cell		{5,3,3}	600	1200	720 pentagons	120 dodecahedra	tetrahedra	600-cell	H_4	14400
600-cell		{3,3,5}	120	720	1200 triangles	600 tetrahedra	icosahedra	120-cell	H_4	1440

onvex regular 4-polytopes					
pentachoron	tesseract	16-cell	24-cell	120-cell	600-cell
{3, 3, 3}	{4, 3, 3}	{3, 3, 4}	{3, 4, 3}	{5, 3, 3}	{3, 3, 5

Bibliography

Sphere packing, helices and the polytope {3, 3, 5}

E.A. Lord[a] and S. Ranganathan

Dept. of Metallurgy, Indian Institute of Science, Bangalore 560 012, India

Received 27 March 2001

Abstract. The packing of tetrahedra in face contact is well-known to be relevant to atomic clustering in many complex alloys. We briefly review some of the structures that can arise in this way, and introduce methods of dealing with the geometry of the polytope {3, 3, 5}, which is highly relevant to an understanding of these structures. Finally, we present a method of projection from S_3 to E_3 that enables coordinates for the key vertices of the collagen model of Sadoc and Rivier to be calculated.

Regular Polytopes, Root Lattices, and Quasicrystals*

R. Bruce King

Department of Chemistry, University of Georgia, Athens, Georgia 30602, USA
(E-mail: rbking@sunchem.chem.uga.edu.)

RECEIVED APRIL 1, 2003; REVISED JULY 8, 2003; ACCEPTED JULY 10, 2003

The icosahedral quasicrystals of five-fold symmetry in two, three, and four dimensions are related to the corresponding regular polytopes exhibiting five-fold symmetry, namely the regular pentagon (H_2 reflection group), the regular icosahedron {3,5} (H_3 reflection group), and the regular four-dimensional polytope {3,3,5} (H_4 reflection group). These quasicrystals exhibiting five-fold symmetry can be generated by projections from indecomposable root lattices with twice the number of dimensions, namely $A_4 \rightarrow H_2$, $D_6 \rightarrow H_3$, $E_8 \rightarrow H_4$. Because of the subgroup relationships $H_2 \subset H_3 \subset H_4$, study of the projection $E_8 \rightarrow H_4$ provides information on all of the possible icosahedral quasicrystals. Similar projections from other indecomposable root lattices can generate quasicrystals of other symmetries. Four-dimensional root lattices are sufficient for projections to two-dimensional quasicrystals of eight-fold and twelve-fold symmetries. However, root lattices of at least six-dimensions (*e.g.*, the A_6 lattice) are required to generate two-dimensional quasicrystals of seven-fold symmetry. This might account for the absence of seven-fold symmetry in experimentally observed quasicrystals.

Key words
polytopes
root lattices
quasicrystals
icosahedron

John Baez on H3 and H4 in a weekly talk.

Contact

The author may be reached at

Jaq 2013 at out look dot com all of this connected with no spaces

“Some men see things and ask, why? I dream of things that never were and I ask, why not?”

Robert Francis Kennedy (RFK), after George Bernard Shaw